NOAA Technical Report NESDIS 121

Calibration of the Advanced Microwave Sounding Unit-A Radiometer for METOP-A

Washington, D.C.
August 2006

U.S. DEPARTMENT OF COMMERCE
National Oceanic and Atmospheric Administration
National Environmental Satellite, Data, and Information Service

NOAA TECHNICAL REPORTS

National Environmental Satellite, Data, and Information Service

The National Environmental Satellite, Data, and Information Service (NESDIS) manages the Nation's civil Earth-observing satellite systems, as well as global national data bases for meteorology, oceanography, geophysics, and solar-terrestrial sciences. From these sources, it develops and disseminates environmental data and information products critical to the protection of life and property, national defense, the national economy, energy development and distribution, global food supplies, and the development of natural resources.

Publication in the NOAA Technical Report series does not preclude later publication in scientific journals in expanded or modified form. The NESDIS series of NOAA Technical Reports is a continuation of the former NESS and EDIS series of NOAA Technical Reports and the NESC and EDS series of Environmental Science Services Administration (ESSA) Technical Reports.

A limited number of copies are available by contacting Jessica Pejsa, NOAA/NESDIS, E/RA3, 5200 Auth Road, Room 601, Camp Springs, Maryland 20746, (301) 763-8184 x115. Copies can also be ordered from the National Technical Information Service (NTIS), U.S. Department of Commerce, Sills Bldg., 5285 Port Royal Road, Springfield, VA 22161, (703) 487-4650 (prices on request for paper copies or microfiche, please refer to PB number when ordering). A partial listing of more recent reports appear below:

NESDIS 93 GOES Imager and Sounder Calibration, Scaling, and Image Quality. Donald W. Hillger, June 1999.

NESDIS 94 MSU Antenna Pattern Data. Tsan Mo, Thomas J. Kleespies, and J. Philip Green, March 2000.

NESDIS 95 Preliminary Findings from the Geostationary Interferometer Observing System Simulation Experiments (OSSE). Bob Aune, Paul Menzel, Jonathan Thom, Gail Bayler, Allen Huang, and Paolo Antonelli, June 2000.

NESDIS 96 Hydrography of the Ross Sea Continental Shelf During the Roaverrs, NBP96-06, Cruise December 1996 - January 1997. Michael L. Van Woert, David Pryor, Eric Quiroz, Richard Slonaker, and William Stone, September 2000.

NESDIS 97 Hydrography of the Ross Sea Continental Shelf During the Roaverrs, NBP97-09, Cruise December 1997 - January 1998. Michael L. Van Woert, Lou Gordon, Jackie Grebmeier, Randal Holmbeck, Thomas Henderson, and William F. Van Woert, September 2000.

NESDIS 98 NOAA-L and NOAA-M AMSU-A Antenna Pattern Corrections. Tsan Mo, August 2000.

NESDIS 99 The Use of Water Vapor for Detecting Environments that Lead to Convectively Produced Heavy Precipitation and Flash Floods. Rod Scofield, Gilberto Vicente, and Mike Hodges, September 2000.

NESDIS 100 The Resolving Power of a Single Exact-Repeat Altimetric Satellite or a Coordinated Constellation of Satellites: The Definitive Answer and Data Compression. Chang-Kou Tai, April 2001.

NESDIS 101 Evolution of the Weather Satellite Program in the U.S. Department of Commerce - A Brief Outline. P. Krishna Rao, July 2001.

NOAA Technical Report NESDIS 121

Calibration of the Advanced Microwave Sounding Unit-A Radiometer for METOP-A

Tsan Mo
NOAA/NESDIS/ORA
5200 Auth Road, WWB/810
Camp Springs, MD 20746

Washington, DC
August 2006

U.S. DEPARTMENT OF COMMERCE
Carlos M. Gutierrez, Secretary

National Oceanic and Atmospheric Administration
Vice Admiral Conrad C. Lautenbacher, Jr., U.S. Navy (Ret.), Under Secretary

National Environmental Satellite, Data, and Information Service
Gregory W. Withee, Assistant Administrator

TABLE OF CONTENTS

TABLE CAPTIONS

FIGURE CAPTIONS

CALIBRATION OF THE ADVANCED MICROWAVE SOUNDING UNIT-A RADIOMETER FOR METOP-A

Tsan Mo
NOAA/NESDIS
Office of Research and Applications
5200 Auth Road, Camp Springs, MD 20746

ABSTRACT

After successful launches of the Advanced Microwave Sounding Unit-A (AMSU-A) onboard the NOAA-K, -L, -M, and -N satellites, receptively, in 1998, 2000, 2002, and 2005, the fifth AMSU-A will be launched onboard the European Organization for the Exploitation of Meteorological Satellites (EUMETSAT) METeorological OPerational (METOP) in October 2006. This report concerns the analysis and evaluation of the thermal-vacuum chamber calibration data from the AMSU-A1 SN 106 and AMSU-A2 SN 108 flight models (FM) for METOP-A. These pre-launch calibration data were analyzed to evaluate the instrument performance, including calibration accuracy, nonlinearity, and temperature sensitivity. Great effort was taken to understand the instrument's radiometric performance as a function of instrument temperature. The calibration data provide a base for derivation of the calibration parameters input data sets (CPIDS) which will be incorporated into the operational calibration algorithms for producing the AMSU-A 1B data sets. NOAA and EUMETSAT has agreed that a common CPIDS will be used at both agencies.

The nonlinearity parameters, which will be used for correcting the nonlinear contributions from an imperfect square-law detector, were determined from this data analysis. The existence and magnitude of nonlinearity in each channel were established and simulated with a quadratic formula for modeling the nonlinear contribution that was developed in the analysis of the NOAA-KLMN AMSU-A pre-launch calibration data. The model was characterized by a single parameter u, values of which were obtained for each channel via least-squares fit to the data. Quadratic corrections which would be expected from the on-orbit data after the launch of AMSU-A into space were simulated. In these simulations, the cosmic background radiance corresponding to a cold space temperature 2.73K was adopted as one of the two reference points of calibration. The largest simulated nonlinear correction is about 2 K. Experience learned from examining the previous AMSU-A on-orbit data provides a better understanding of the AMSU-A performance in space and helps process these pre-launch calibration data. The calibration information presented in this report will be useful for post launch on-orbit verification of the AMSU-A instrument performance.

1. INTRODUCTION

On 13 May 1998, the NOAA-K, which is designated NOAA-15 after the launch, was successfully launched into a circular, near-polar orbit with an altitude of 833-km above the Earth and an inclination angle of 98.7° to the Equator. NOAA-15 carries the first of a series of new microwave total-power radiometers, the Advanced Microwave Sounding Units (AMSU-A and AMSU-B), which provide 20 channels for atmospheric temperature and moisture soundings. NOAA-L/16, which was launched on September 28, 2000, carries the second AMSU-A. The NOAA-M/17 AMSU-A was successfully launched on June 24, 2002. NOAA-17 is the first NOAA satellite that has been launched into an orbit to cross the Equator at 1000 and 2200 local time. NOAA-N/18, which was launched on May 20, 2005, carried the first Microwave Humidity Sounder (MHS) which replaces AMSU-B for humidity sounding.

The AMSU-A is divided into two physically separate modules, each of which operates and interfaces with the spacecraft independently. The AMSU-A1 module uses two independent antenna-radiometer systems (A1-1 and A1-2) to provide 12 channels in the range 50.3 to 57.3 GHz oxygen band for retrieving the atmospheric temperatures from the Earth's surface to about 50 kilometers (or 1 mb), and another channel at 89 GHz. The AMSU-A2, which has 2 channels at 23.8 and 31.4 GHz, are used to identify precipitation and correct the effect of surface emissivity, atmospheric liquid water, and water vapor on temperature sounding. These window channels are also used to derive rain rate, sea ice concentration, and snow cover.

Table 1 lists some of the METOP AMSU-A main channel characteristics, including channel frequency, number of bands, 3-dB RF band width, radiometric temperature sensitivity (or NEΔT), antenna beam efficiency, polarization, and field of view (FOV) of angular beam width for each channel. More detailed information on the AMSU-A radiometers is reported elsewhere [1]. Each of the AMSU-A antenna systems has a nominal FOV of 3.3° at the half-power points and covers a cross-track scan of $\pm 48°20'$ (to beam centers) from the nadir direction with 30 Earth FOVs per scan line. Beam positions 1 and 30 are the outermost scan positions of the Earth views, while beam positions 15 and 16 (at $\pm 1.67°$ from nadir) straddle the nadir. Views of cold space and a black-body target at the end of a scan provide onboard calibration once every 8 seconds.

EUMETSAT provides the Microwave Humidity Sounder (MHS) for humidity sounding. It has two channels at 89 and 157 GHz, respectively, two channels around the 183 GHz water vapor line, and another channel at 190 GHz. Detailed description of the MHS radiometric performance has been

given elsewhere [2].

All of the AMSU-A flight models were tested and calibrated in a thermal-vacuum (TV) chamber by the contractor. These pre-launch TV calibration data were evaluated and analyzed to derive the calibration parameters input data set (CPIDS) which is used in the NOAA operational calibration algorithm to produce the AMSU-A 1B data sets. Particularly, there is a small nonlinearity (of the order of 1 K or less), which cannot be evaluated by the two-point calibration but is determined from the pre-launch calibration data.

In this study, the TV test data from the METOP-A AMSU-A instruments are analyzed and evaluated. The same procedure developed for NOAA-K AMSU-A calibration [1] is closely followed. Experience gained from examining the NOAA-15 and NOAA-16 AMSU-A on-orbit data provides a better understanding of the AMSU-A performance in space and helps improve the analysis of the pre-launch calibration data.

In the following sections, the results from the data analysis are presented. Instrument performances evaluated in this analysis include calibration accuracy, nonlinearity, and radiometric temperature sensitivity (or NEΔT, the noise-equivalent temperature). Section 1 gives an introduction and section 2 presents a brief description of the TV chamber test data. The calibration algorithm is described in section 3. The results are presented in section 4. Conclusion and discussion are in section 5. Tables of CPIDS for METOP-A AMSU-A are given in Appendices A. A brief description of the NOAA Level 1B data is given in Appendix B.

2. DESCRIPTION OF CALIBRATION DATA

Aerojet (now Northrop Grumman), the AMSU-A contractor, took the calibration data in a TV test chamber using the full scan mode. In this mode, AMSU-A scans through 30 Earth FOVs, the cold target, and the internal warm blackbody target once every 8 seconds. It takes one sample at each Earth FOV and two samples at the cold and warm targets, respectively. Since the scene calibration target was fixed at FOV 6 ($31^{\circ}40'$ from nadir), only radiometric counts from FOV 6 are used for calibration. Each antenna system looks at its own individual cold, warm, and scene targets. A series of Platinum Resistance Thermometers (PRTs) were used to monitor the temperatures of these calibration targets. The numbers of PRTs used to measure the physical temperatures of the scene, cold, and warm calibration targets in each antenna system are given in

Table 1. METOP-A AMSU-A1 SN 106 and AMSU-A2 SN 108 Channel Characteristics.

Channel Number	Channel Frequency (MHz)		No. of Bands	Measured 3-dB RF Bandwidth (MHz)	NEΔT (K)		Beam[b] Efficiency	Polarization (NADIR)	FOV[c] (deg.)
	Specification	Measured[a]			Spec.	Measured			
1	23800	23800.80	1	251.98	0.30	0.191	97%	V	3.53
2	31400	31400.44	1	159.98	0.30	0.229	98%	V	3.32
3	50300	50300.40	1	160.72	0.40	0.261	96%	V	3.37
4	52800	52800.27	1	379.96	0.25	0.149	96%	V	3.39
5	53596 ± 115	53596.50 ± 115	2	167.75 | 167.75	0.25	0.177	95%	H	3.41
6	54400	54400.69	1	380.40	0.25	0.142	97%	H	3.46
7	54940	54939.86	1	380.16	0.25	0.140	97%	V	3.39
8	55500	55500.09	1	310.26	0.25	0.180	96%	H	3.38
9	fo = 57290.344	fo = 57290.325	1	309.78	0.25	0.192	96%	H	3.41
10	fo ± 217	fo ± 217	2	75.87 | 75.87	0.40	0.241		H	
11	fo ± 322.2 ± 48	fo ± 322.2 ± 48	4	34.89 /35.38 |35.38 /34.89	0.40	0.280		H	
12	fo ± 322.2 ± 22	fo ± 322.2 ± 22	4	15.43 / 15.48 | 15.48 / 15.43	0.60	0.388		H	
13	fo ± 322.2 ± 10	fo ± 322.2 ± 10	4	7.81 / 7.86 | 7.86 / 7.81	0.80	0.559		H	
14	fo ± 322.2 ± 4.5	fo ± 322.2 ± 4.5	4	2.93 / 2.94 | 2.94 / 2.93	1.20	0.916		H	
15	89000	88997yghn.00	1	1996.54	0.50	0.108	97%	V	3.49

[a]At a temperature of 20° C for channels 1, 2, and 15; at 22° C for other channels.
[b]Measured.
[c]Specification is 3.3° ± 10%.

Table 2. Number of PRTs in each calibration target and channels provided by individual antenna systems. The last row gives the number of scans collected in the calibration for each system

Items	Number of PRTs in each target			Remarks
	A2	A1-2	A1-1	
Warm Target	7	5	5	
Cold Target	11	7	7	
Scene Target	11	7	7	
Channels	1 & 2	3, 4, 5 & 8	6, 7, & 9-15	
PLLO#2	-	-	Ch. 9-14	Backup PLLO
N(Scan No.)	120	400 to 900	400 to 900	See Note

Note: For A1-1 & A1-2: N=400, 400, 550, 725, 725, and 900 when the scene target temperature at T_s=84, 130, 180, 230, 280, and 330K, respectively.

Table 2 which also lists the channels provided by each AMSU-A antenna system. Channels 9-14 have both primary and secondary phase locked loop oscillators (i.e. zPLLO #1 and PLLO #2, respectively) built-in. The PLLO #2 will be used for backup if PLLO #1 fails in operation. Invar high-Q cavity stabilized local oscillators [3] are used in other channels.

The physical temperatures of scene and cold targets measured by individual PRTs were provided in Kelvin (K) on Aerojet's data packages. However, the data from the PRTs monitoring the warm blackbody targets are given in counts, which are proportional to the blackbody temperatures. One should note that the scene and cold targets used in the TV chamber will not be carried into space. The PRT counts from the warm blackbody targets must be converted to PRT temperatures. The normal approach of deriving the PRT temperatures from counts is a two-step process: (1) the resistance of each PRT in ohms is computed by a count-to-resistance look-up table provided by the manufacturer. In this study, we used a polynomial representation of the count-to-resistance relationship provided by Aerojet; and (2) the individual PRT temperature in degrees Celsius is obtained from an analytic PRT equation [4], which is described in Appendix A. However, the two steps can be compressed to a single step with negligible errors. This single step process, which has been used in the NOAA-KLMN calibrations, computes the PRT temperatures directly from the PRT counts, using a cubic polynomial

$$T_{Wk} = \sum_{j=0}^{3} f_{kj} C_k^j \quad (1)$$

where T_{Wk} and C_k represent the temperature and count of the PRT k. The polynomial coefficients, f_{kj}, are derived for each PRT in this study. Equation (1) also applies to 47 other housekeeping temperature sensors, such as the mixers, the IF amplifiers and the local oscillators. These f_{kj} coefficients for all PRTs and housekeeping sensors in METOP AMSU-A1 SN 106 and AMSU-A2 SN 108 are listed in Appendix A (Tables A-1 and A-2, respectively).

The mean internal blackbody temperature, T_W, is calculated from the individual PRT temperatures,

$$T_W = \frac{\sum_{k=1}^{m} W_k T_{Wk}}{\sum_{k=1}^{m} W_k} + \Delta T_W \quad (2)$$

where m represents the number of PRTs for each antenna system (as listed in Table 2) and W_k is a weight assigned to each PRT k. The quantity ΔT_W is a warm load correction factor, which is derived for each channel from the TV test data at three instrument temperatures (low, nominal, and high). The procedure for determining the ΔT_W values has been described elsewhere [5]. For each AMSU-A antenna system, a special set of calibration data was taken to determine the ΔT_W values, which are given in Appendix A (Table A-3). The W_k value, which equals 1 (0) if the PRT k is determined good (bad) before launch. Similarly, the mean temperatures of cold targets are defined in the same way as in Equation (2), except without the term ΔT_W.

The TV calibration data were taken at three instrument temperatures and the scene target was cycled through six temperatures 84, 130, 180, 230, 280, and 330K, respectively, at each instrument temperature. At each of the scene target temperatures, calibration data were acquired for enough number of scans to assure an effective temperature sensitivity less than 0.03K. The number of scans required depends upon the expected NEΔT of channel 14 (which has the largest NEΔT) and is therefore a function of the scene target temperature. Actual numbers of scans taken at individual temperatures are given in Table 2. The uncertainties in knowledge of brightness temperatures and measurement errors were obtained by Aerojet [6, 7]. These are given Table 3.

Table 3. Uncertainty in brightness temperatures and measurement errors.

Source of Error	AMSU-A2 :Ch. 1 and 2		AMSU-A1: Ch. 3 - 15	
	Bias (K)	Random (k)	Bias (K)	Random (k)
Warm Target	-0.050	±0.122	-0.050	±0.122
Cold Target	0.024	±0.105	0.024	±0.091
Scene Target	0.002	±0.101	0.002	±0.090

Antenna beam widths at all channels were also measured and the values for METOP-A are listed in Table 1. Antenna beam efficiency was calculated at each channel frequency and is listed in Table 1.

3. CALIBRATION ALGORITHM

In this study, calculations of radiometric measurements and variables related to the calibration process are all performed in radiance with dimension of mW/(m^2-sr-cm^{-1}), but the final results are presented in temperatures. All instruments flown on NOAA satellites produce measurements in radiance. Conversion between brightness temperature and radiance was performed using the full Planck function, instead of the Rayleigh-Jeans approximation. This also eliminates any possible conversion inaccuracy that may occur, particularly in the region of the space cosmic back-ground temperature ~2.73K, where the Rayleigh-Jeans approximation breaks down.

For each scan, the blackbody radiometric counts C_W are the averages of two samples of the internal blackbody. Similarly, the space radiometric counts C_C are the average of two samples of the space target. To reduce noise in the calibrations, the C_X (where X=W or C) for each scan line were convoluted over several neighboring scan lines according to the weighting function [1]

$$\overline{C}_X = \frac{\sum_{i=-n}^{n} W_i C_X(t_i)}{\sum_{i=-n}^{n} W_i} \qquad (3)$$

where t_i (when $i \neq 0$) represents the time of the scan lines just before or after the current scan line and

t_0 is the time of the current scan line. One can write $t_i = t_0 + i\Delta t$, where $\Delta t = 8$ seconds for AMSU-A. The 2n+1 values are equally distributed about the scan line to be calibrated. Following the NOAA-KLM operational preprocessor software, the value of n=3 is chosen for all AMSU-A antenna systems. A set of triangular weights of 1, 2, 3, 4, 3, 2, and 1 is chosen for the weight factor W_i that appears in Equation (3) for the seven scans with i = -3, -2, -1, 0, 1, 2, and 3.

The calibration algorithm [1], which takes into account the nonlinear contributions due to an imperfect square-law detector, converts scene counts to radiance R_S as follows,

$$R_S = R_W + \left(R_W - R_C\right)\left(\frac{C_S - \overline{C}_W}{\overline{C}_W - \overline{C}_C}\right) + Q \tag{4}$$

where R_W and R_C are the radiance computed from the PRT blackbody temperature T_W and the PRT cold target temperature T_C, respectively, using the Planck function. The C_S is the radiometric count from the Earth scene target. The averaged blackbody and space counts, $\overline{C}_W$ and $\overline{C}_C$, are defined by Equation (3).

The quantity Q, which represents the nonlinear contribution, is given by [1]

$$Q = u\left(R_W - R_C\right)^2 \frac{\left(C_S - \overline{C}_W\right)\left(C_S - \overline{C}_C\right)}{\left(\overline{C}_W - \overline{C}_C\right)^2} \tag{5}$$

where u is a free parameter, values of which are determined at three instrument temperatures (low, nominal, and high). After launch, the u values at the actual on-orbit instrument temperatures will be interpolated from these three values. For channels 9-14 (AMSU-A1-1), two sets of the u parameters are provided; one set is for the primary PLLO#1 and the other one for the redundant PLLO#2.

The quantity R_S in Equation (4) represents the radiometric scene radiance of individual channels. For users of NOAA Level 1B data, a simplified formula, which converts C_S directly into R_S, is presented in Appendix B. It should be noted that the ratios in Equations (4) and (5) will eliminate the effect of any linear variation in the radiometric counts on R_S. The channel gain, G, is defined as

$$G = \frac{\overline{C}_W - \overline{C}_C}{R_W - R_C} \tag{6}$$

The quantity G varies with instrument temperature, which is defined as the RF Shelf temperature for each AMSU-A antenna system. For a fixed instrument temperature, G is approximately constant. The first two terms in Equation (4) constitute a linear two-point calibration equation, if the quadratic term is negligible. Let R_{SL} denote these two terms,

$$R_{SL} = R_W + \left(R_W - R_C\right)\left(\frac{C_S - \overline{C}_W}{\overline{C}_W - \overline{C}_C}\right) \tag{7}$$

The linear scene radiances R_{SL} are calculated using the TV chamber test data. The results are discussed in the following section.

4. RESULTS

4.1 *Calibration Accuracy*

The calibration accuracy, R, is defined as the difference between the scene PRT radiance R_{sprt} and the radiometric scene radiance. It is calculated from the equation

$$\Delta R = \frac{1}{N}\left[\sum_{i=1}^{N}\left(R_{sprt} - R_{SL}\right)_i\right] \tag{8}$$

where N is the number of scans at a specific scene temperatures (N= 120 for AMSU-A2 channels but ranging from 400 to 900 for AMSU-A1 channels).

Equation (7) would be a good representation of the microwave radiometric scene radiance for a perfect square-law detector. Any deviation of the quantity R_{SL} from the measured scene PRT radiance R_{sprt} indicates the presence of either nonlinearity in the radiometer system or some other potential source of contamination in the calibration data.

Figure 1 shows the calculated calibration accuracies in temperature, ΔT (corresponding to ΔR), versus the scene PRT temperature for channels 1 through 15. The AMSU-A specification requires ΔT = 2.0K for channels 1, 2, and 15, and ΔT = 1.5K for all other channels. The results in Figure 1 are better than the specification at all channels.

4.2 *Nonlinearity*

The ΔT patterns (Figure 1) show clearly the nonlinearity patterns which can be represented by the quadratic formula Q defined in Equation (5). The nonlinearity of a channel is normally defined as the residuals from a least-squares fit of its scene PRT radiance as a linear function of the radiometric radiance R_{SL} (Equation 7). The nonlinearity is defined as the differences (or residuals) between the R_{sprt} and the best-fit results from a linear equation in the form LinFit = a + bR_{SL} (where a and b are the intercept and slope). These residuals, which are defined as the measured nonlinearity Q (= R_{sprt} - LinFit), are shown in Figure 2. The largest (absolute) Q value on each curve is defined as the measured nonlinearity that can be compared to those as defined in the AMSU-A specification.

The results in Figure 2 show that the maximum (absolute) Q values are about 0.6K. The AMSU-A specification requires Q = 0.5K for channels 1, 2, and 15; and Q = 0.375K for other channels. All results at AMSU-A1-1 channels in Figure 2 do not meet the specifications. All of the curves, except channel 2, in Figure 2 have two roots, representing solutions of a quadratic equation, which can be written in the form

$$Q = u\left(R_S - R_1\right)\left(R_S - R_2\right) \tag{9}$$

where R_1 and R_2 represent the two roots. One can obtain a similar equation from Equation (5) by replacing the counts by its individual radiance, since the radiometric counts are proportional to radiance in a first-order approximation. The resultant equation represents a different straight line intersecting the same curve at R_W and R_C. Once the parameter u is determined, it can be used with any pair of roots to calculate Q. We applied Equation (9) to fit the quadratic curves in Figure 2 to obtain the u values with the two roots extracted from each plot. Table 4 gives the best-fit u values at three instrument temperatures for individual channels.

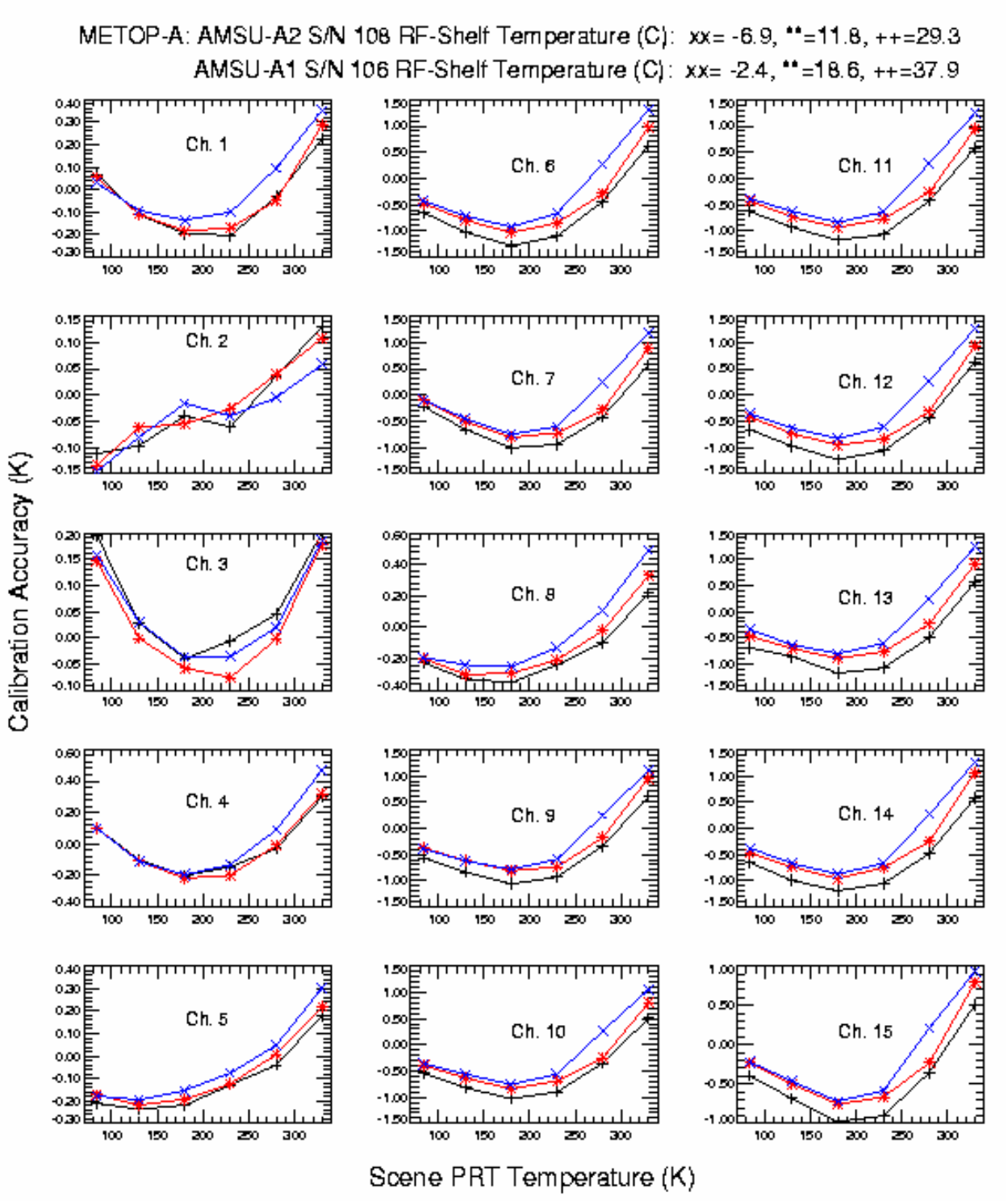

Figure 1. METOP-A AMSU-A: Calibration accuracies at three instrument temperatures.

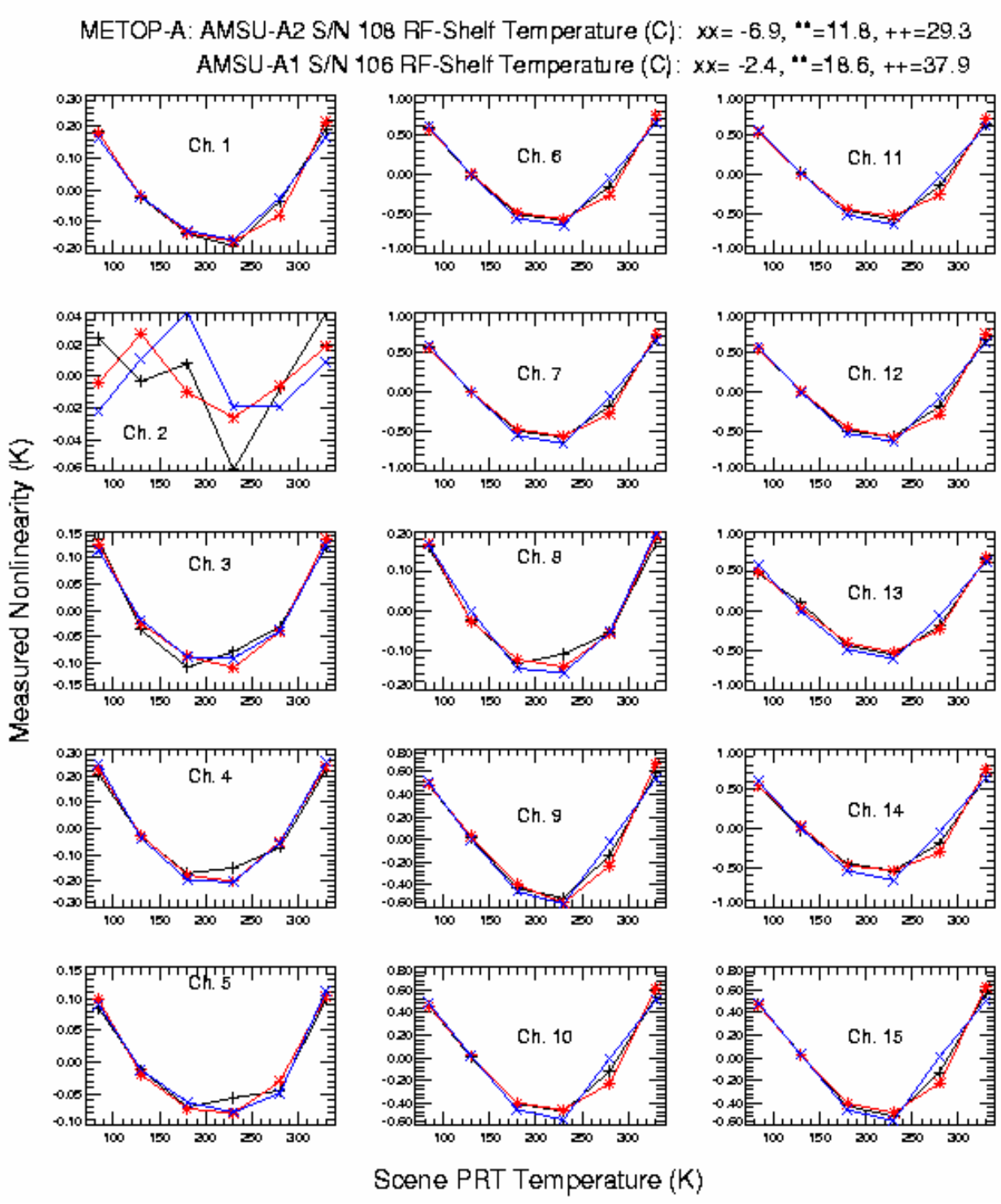

Figure 2. METOP-A AMSU-A: Pre-launch measured nonlinearities at three instrument temperatures.

4.3 Simulated Quadratic Corrections to On-Orbit Data

Once the u values are determined, Equation (9) can be used to simulate the quadratic contributions which are expected from on-orbit data. This can be accomplished by replacing the roots R_1 and R_2 with the radiance $R_{2.73}$ (corresponding to cold space temperature 2.73K) and R_W, respectively. The simulated results are shown in Figure 3 for all channels at three instrument temperatures which are listed at the top of the plots. One should note that the instrument temperatures are different for the three AMSU-A antenna systems. The simulated quadratic contributions displayed in Figure 3 are larger than those shown in Figure 2. This is expected because the separation of the two reference calibration points is increased in the cases of simulations. Noticeable quadratic contributions appear in all channels, particularly the AMSU-A1-1 channels. The largest ones are approximately 1.8 K at several channels. It is important to note that the effect of instrument temperature on the quadratic contributions is nonlinear in general.

Similarly, Figure 4 shows the calculated results which are associated with the redundant PLLO#2 built into channels 9-14. The left column of Figure 4 displays the calibration accuracies, ΔT, which are similar to Figure 1 and the middle column (corresponding to Figure 2) shows the residuals of the least-squares fit. The right column shows the simulated quadratic corrections, Q, which would occur in on-orbit data.

Table 4. METOP-A AMSU-A: Nonlinearity parameters u in dimension of (m^2-sr-cm^{-1})/mW.

AMSU-A2 SN 108 channels: **AMSU-A1-2 SN 106 channels:**

Instrument Temp.(C)	Ch. 1	Ch. 2	Instrument Temp.(C)	Ch. 3	Ch. 4	Ch. 5	Ch. 8
-6.91	3.997181	-0.088304	-2.57	0.61973	1.199512	0.459539	0.796928
11.81	4.632821	0.119933	18.53	0.684472	1.116109	0.472265	0.768300
29.29	4.519261	0.440904	38.41	0.659003	1.009618	0.412544	0.708023

AMSU-A1-1 SN 106 channels: PLLO #1

Instrument Temp.(C)	Ch. 6	Ch. 7	Ch. 9	Ch. 10	Ch. 11	Ch. 12	Ch. 13	Ch. 14	Ch. 15
-2.35	2.969043	2.858432	2.212371	2.090453	2.471951	2.553775	2.509132	2.619628	0.848242
18.57	2.939653	2.834368	2.313864	2.138097	2.487536	2.583118	2.313089	2.529191	0.897494
37.88	2.924913	2.791873	2.223045	2.085386	2.404764	2.497221	2.165481	2.459106	0.890082

AMSU-A1-1 SN 106 channels: PLLO #2

Instrument Temp.(C)	Ch. 9	Ch. 10	Ch. 11	Ch. 12	Ch. 13	Ch. 14
-2.36	2.392444	2.141066	2.521564	2.502484	2.266767	2.564267
18.69	2.270486	2.245338	2.698693	2.682700	2.604975	2.748475
37.91	2.359000	2.260214	2.628860	2.631170	2.483230	2.666526

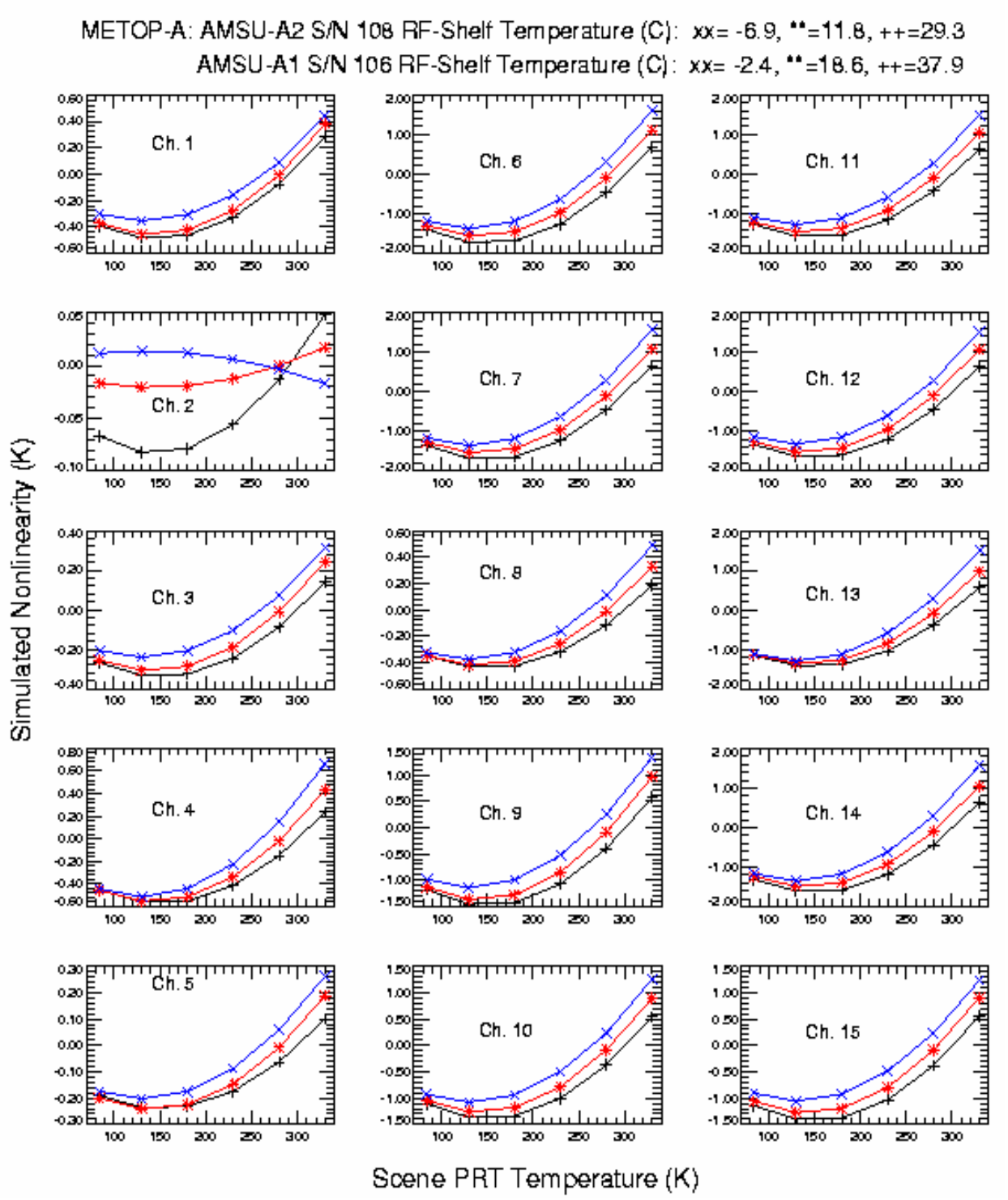

Figure 3. METOP-A AMSU-A: Simulated nonlinearities for on-orbit data.

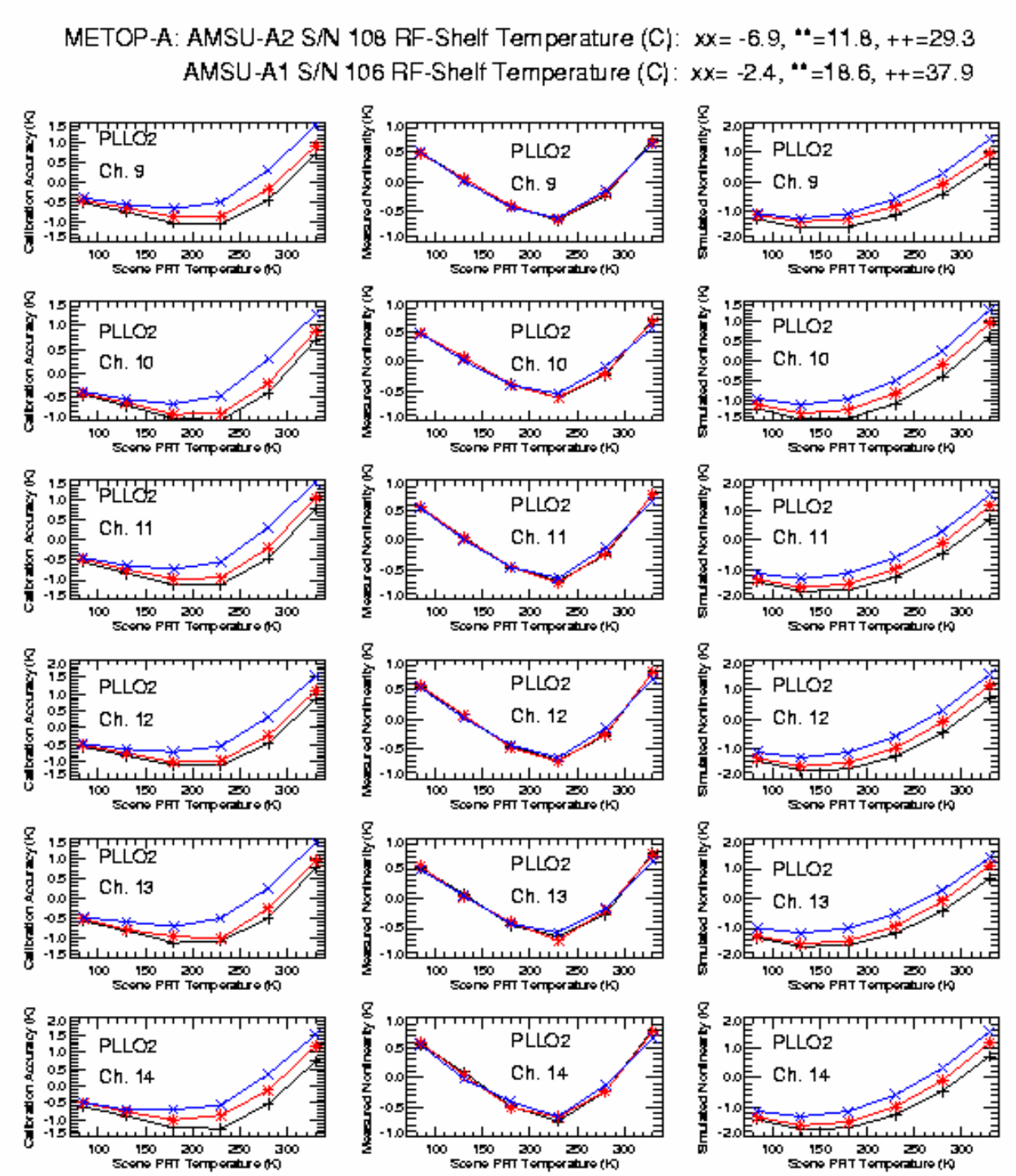

Figure 4. METOP-A AMSU-A: Calibration results with PLLO #2 at Channels 9-14, including calibration accuracy, measured nonlinearity, and simulated on-orbit nonlinearity.

4.4 Temperature Sensitivity

The temperature sensitivity (or NEΔT) specification for AMSU-A channels are listed in Table 1. It is defined as the minimum change of a scene brightness temperature that can be detected. In practice, it is calculated as the standard deviation of the radiometer output (in K), when an antenna system is viewing a scene target at 300K. The calculated NEΔT values are shown in Figure 5 together with the AMSU-A specifications. These calculated NEΔT values correspond to a scene temperature of 300K.. All of the calculated NEΔT values in Figure 5 are better than those given in the AMSU-A specification. Actually, all NEΔT values measured at all temperatures are better than the specification. The calculated NEΔT values at all scene target temperatures and three instrument temperatures are shown in Figure 6. In general, the NEΔT value decreases as the instrument temperature becomes colder.

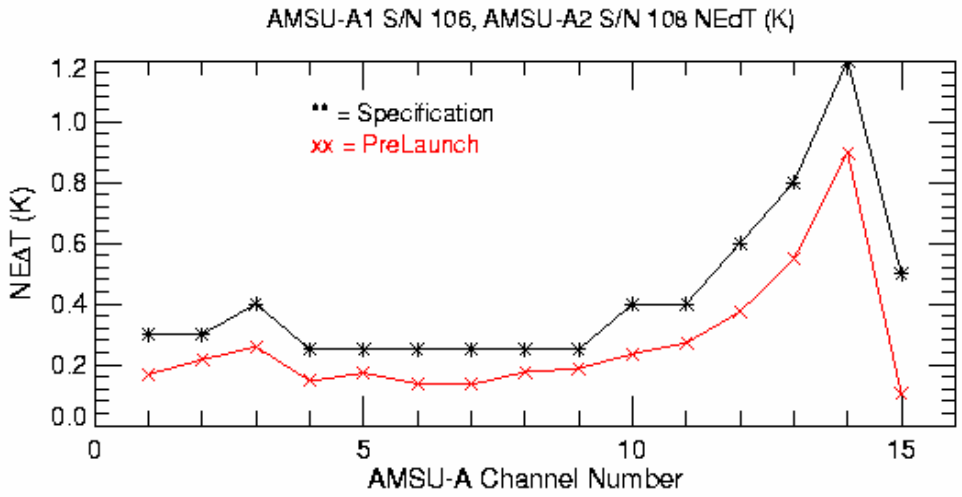

Figure 5. METOP-A AMSU-A: Comparison of the measured NEΔT values with specifications.

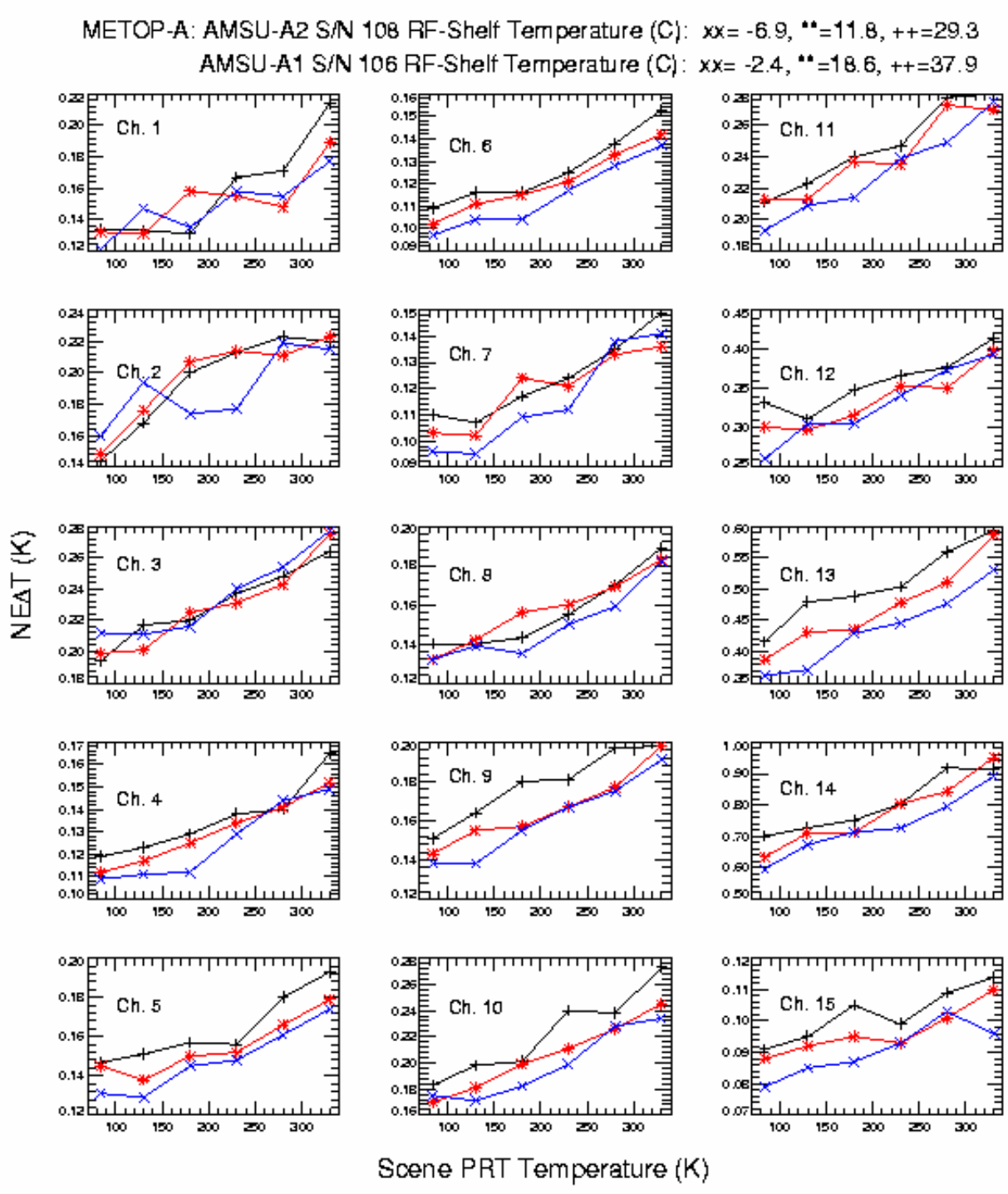

Figure 6. METOP AMSU-A: Measured NEΔT as a function of scene target temperatures at three instrument temperatures.

4.5 Radiometric Counts as a Function of Scene Target Temperature

Figure 7 shows the plots of TV scene radiometric counts versus the scene PRT temperatures for all channels. The radiometric counts increase linearly with scene PRT temperatures ranging from 84 to 330K and good linear relationships exist between the radiometric counts and the scene PRT temperatures in the range 84 to 330K. One can extrapolate these linear relationships to 0 K (corresponding to zero radiance) and obtain the intercepts for these plots. The intercept for each data point can also be computed from Equation (7) by setting R_{SL}= 0 and solve for C_S, which is denoted by C_{Sint} as

$$C_{S\,\mathrm{int}} = \overline{C}_W - G\,R_W \tag{10}$$

where G is the channel gain defined in Equation (6). The calculated C_{Sint} values at three instrument temperatures for each channel are shown in Figure 8. These are the mean values of all calculations performed with all available calibration data (from 120 to 900 scans as the scene temperature varies from 84 to 330K). At each instrument temperature, the variation in the calculated C_{Sint} values is relatively small and all C_{Sint} values are positive. Figure 8 shows that the instrument temperature has a big impact on the magnitude of C_{Sint}, which increases as the instrument temperature decreases, except at channels 3 and 7.

4.6 Channel gains

Values of the channel gains as defined in Equation (6) are also calculated from the TV calibration data. The gain values are converted into dimension of count/K. Figure 9 shows the calculated channel gains at three instrument temperatures, which are listed at the top of Figure 9. One should note that the abnormal behavior of channel 3 gain as a function of instrument temperature. Similarly, Figure 10 shows the calculated results of channel gain, radiometric counts, and intercept counts as a function of the scene PRT temperature when PLLO#2 was used.

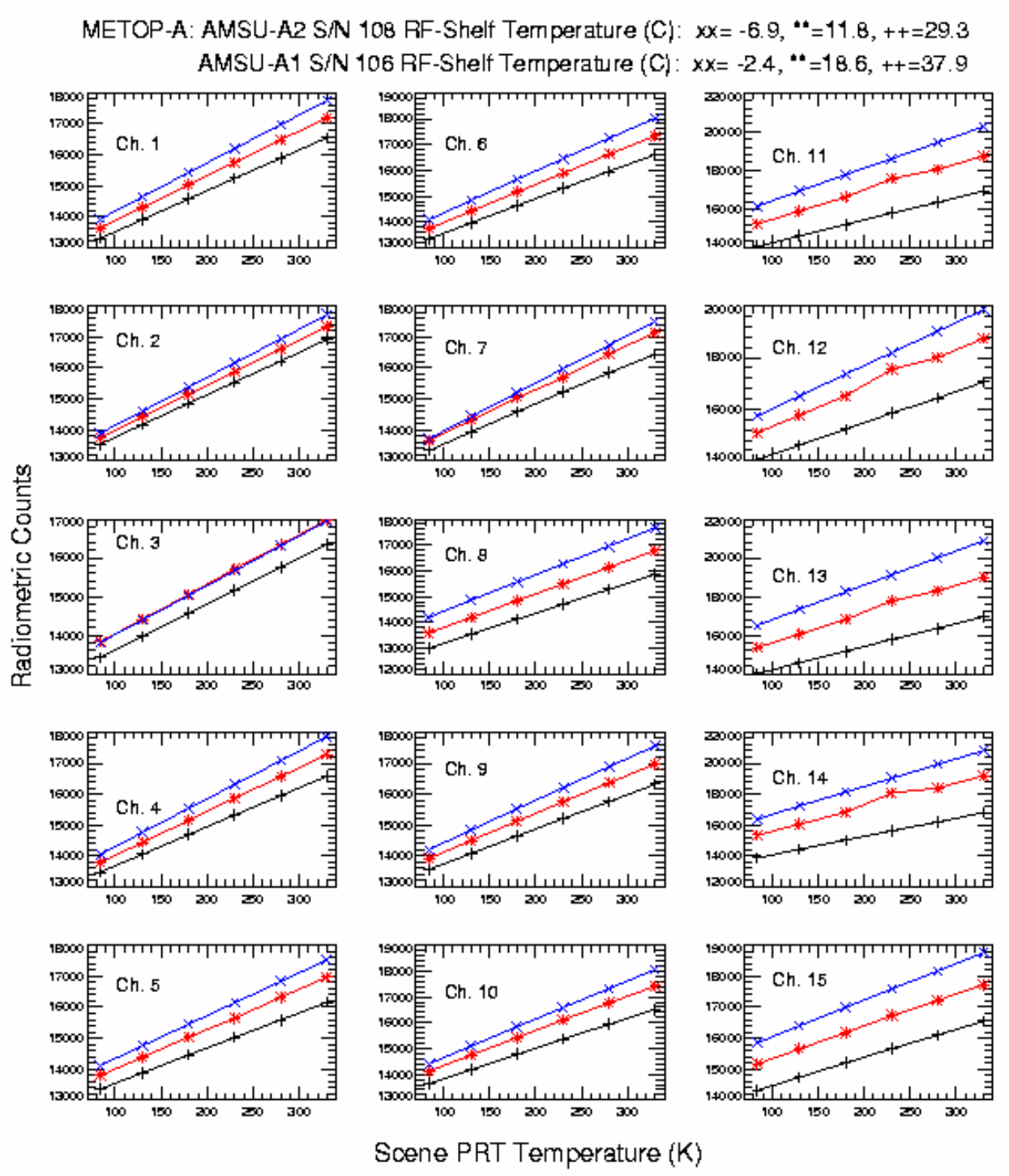

Figure 7. METOP-A AMSU-A: Radiometric counts versus Scene target temeperatures at three instrument temperatures.

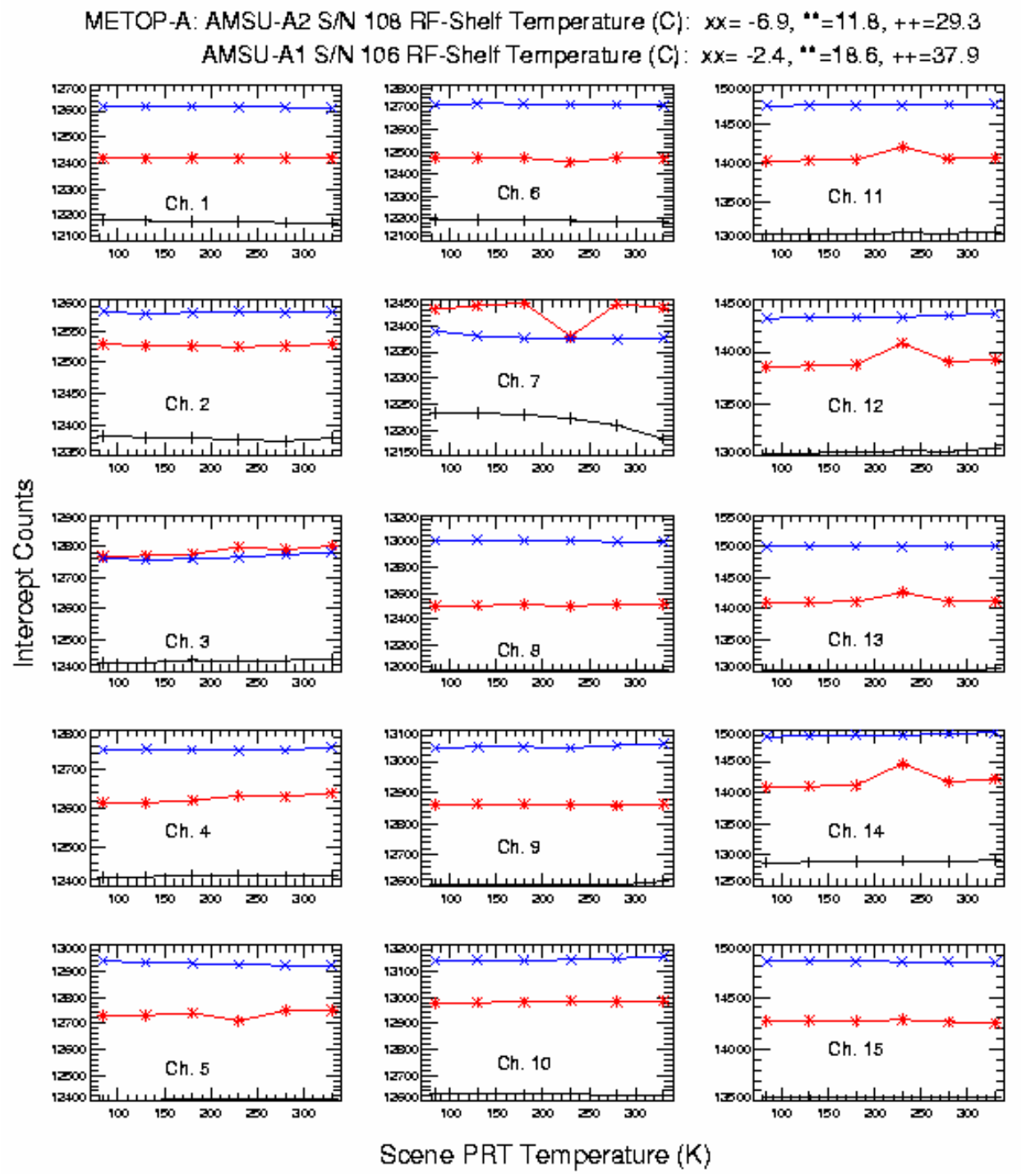

Figure 8. Metop-A AMSU-A: Intercept counts versus Scene target temeperatures at three instrument temperatures.

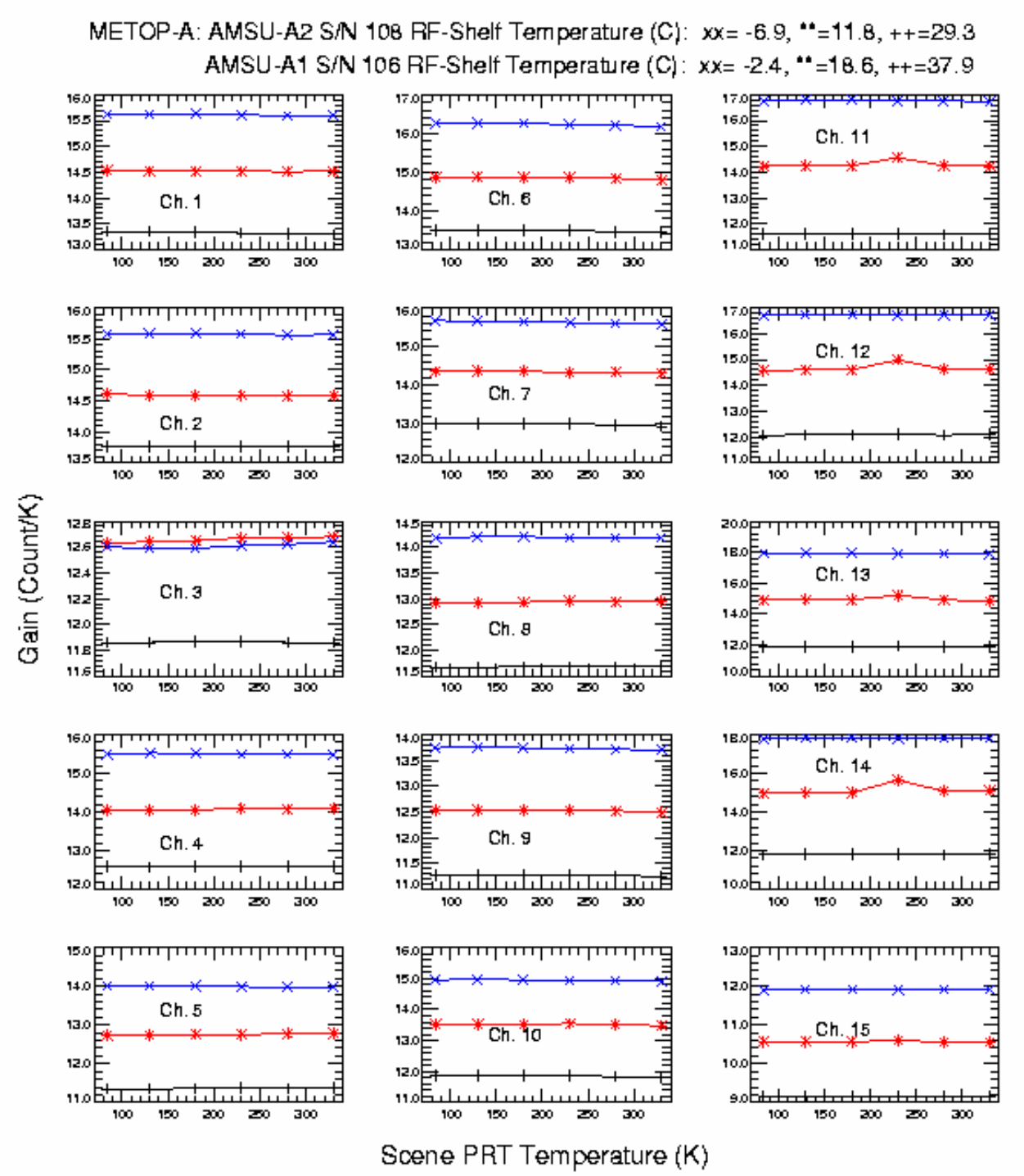

Figure 9. METOP-A AMSU-A: Channels versus Scene target temeperatures at three instrument temperatures.

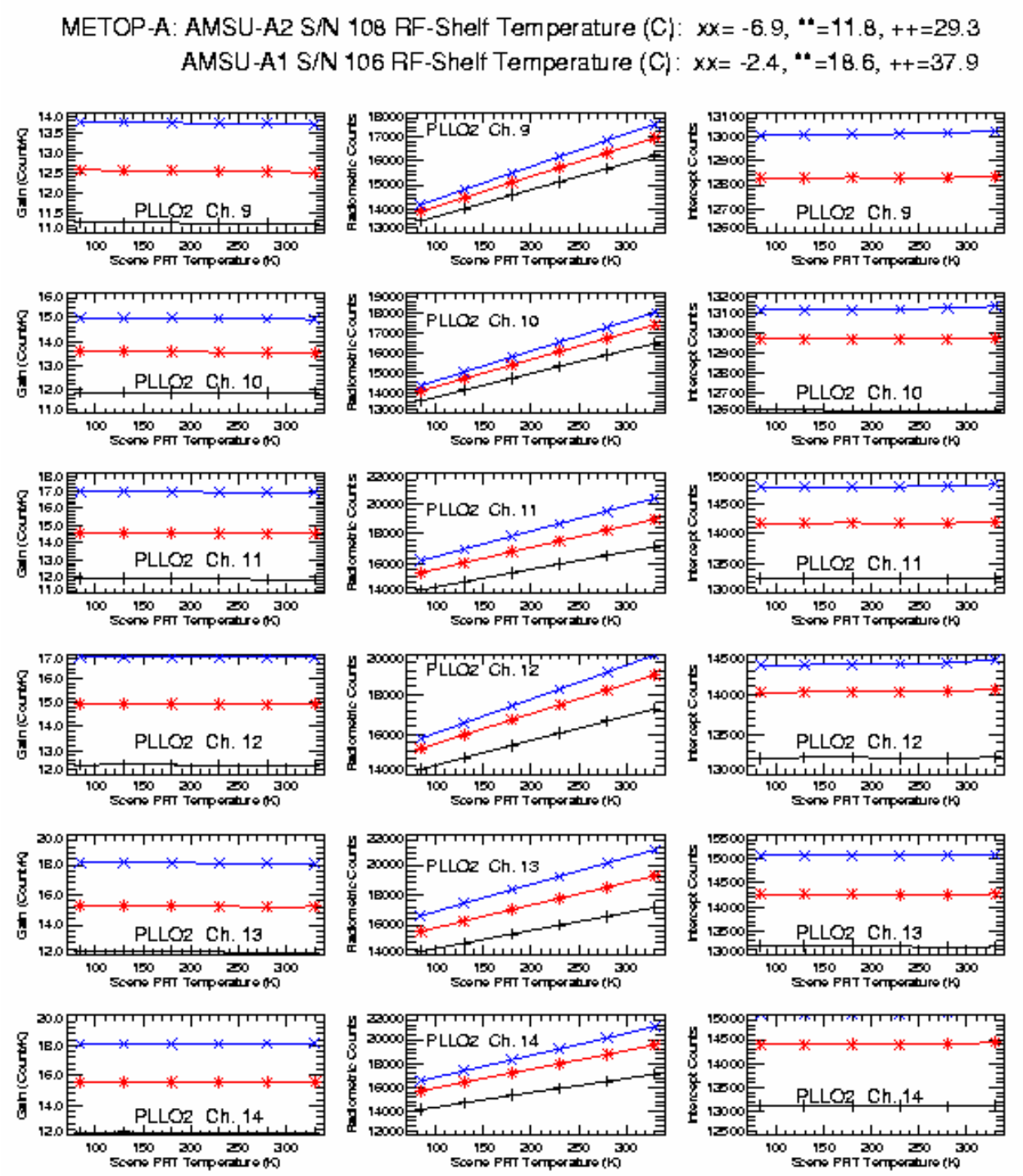

Figure 10. METOP-A AMSU-A: Calibration results with PLLO #2 at Channels 9-14, including gains, radiometric counts, and intercept counts as a function of scene target temperatures at three instrument temperatures..

5. CONCLUSION AND DISCUSSION

The TV chamber calibration data for the METOP AMSU-A, including A1 SN 106 and A2 SN 108, were analyzed to derive the CPIDS which will be used in the NOAA and EUMETSAT operational calibration algorithms to produce the AMSU-A 1B data sets. The results show that the instruments meet the AMSU-A specification in calibration accuracy and temperature sensitivity, but the measured nonlinearities at the AMSU-A1-1 channels do not meet the AMSU-A specification.

The nonlinearity exists at all channels. A quadratic formula with a single parameter u is used to simulate these nonlinear contributions. The u values at three instrument temperatures were obtained from the pre-launch calibration data. Using the best-fit u values, the quadratic corrections which would be expected from the on-orbit data were simulated. In the simulations, the cold space radiance corresponding to 2.73K was adopted as one of the two reference calibration points (the other one is the internal blackbody temperature). The largest simulated nonlinear correction is about 1.8 K as shown in Figure 3.

Experience gained from examining the previous AMSU-A on-orbit data provides a better understanding of the AMSU-A performance in space and helps process the pre-launch calibration data.

In general, the qualities of the calibration data are quite good. Particularly, the instrument temperatures were stabilized at pre-selected values with total variation less than ± 0.5K during each test cycle. This renders the measured instrument nonlinearities more reliable. The results presented in this study confirm the good quality of the AMSU-A instruments for METOP-A. The calibration information presented in this report will be immensely useful for post launch on-orbit verification of the AMSU-A instrument performance.

Acknowledgment

The contents of this manuscript are solely the opinions of the author and do not constitute a statement of policy, decision, or position on behalf of NOAA or the U. S. Government. Aerojet, (now Northrop Grumman) was the primary AMSU-A contractor for building the instruments.

REFERENCES

[1]. Tsan Mo, "Prelaunch Calibration of the Advanced Microwave Sounding Unit-A for NOAA-K," IEEE Trans. Microwave Theory and Techniques, vol. 44, pp. 1460-1469, 1996.

[2]. Tsan Mo and Kenneth Jarva, "Microwave Humidity Sounder Calibration Algorithm," NOAA Technical Report NESDIS 116, October 2004.

[3]. P. K. Patel and J. Mentall, "The Advanced Microwave Sounding Unit-A," in *Microwave Instrumentation for Remote Sensing of the Earth,* SPIE Vol. 135, Orlando, April 13-14, 1993, pp.130-135.

[4]. PRT Handbook, Bulletin 1024, 1986, Rosemount Inc., Burnsville, MN 55337.

[5]. Tsan Mo, "Calibration of the Advanced Microwave Sounding Unit-A for NOAA-K," NOAA Technical Report NESDIS 85, June 1995.

[6]. Calibration Log Book for AMSU-A2 SN 108," Report No. 11329, April 2000, Aerojet, Azusa, CA 91702.

[7]. Calibration Log Book for AMSU-A1 SN 106," Report No. 11324B, May 2004, Northrop Grumman, Azusa, CA 91702.

[8]. Tsan Mo, "AMSU-A Antenna Pattern Corrections," IEEE Trans. Geoscience and Remote Sensing, vol. 37, pp. 103-112, 1999.

APPENDIX A

METOP-A CPIDS : COEFFICIENTS OF AMSU-A1 SN 106 AND AMSU-A2 SN 108

A.1 *Polynomial Coefficients for Converting PRT Counts into Temperatures*

The two-step process for deriving the PRT temperatures from PRT counts C_k is briefly described here. First the count C_k from PRT k is converted into resistance r_k (in ohms) by a polynomial

$$r_k = \sum_{i=0}^{3} A_i C_k^i \tag{A-1}$$

where the coefficients A_i for individual PRTs and temperature sensors were provided by Aerojet. Once the resistance r_k is known, then one can calculate the PRT temperature t (in Celsius) from the Callendar-Van Dusen equation [6], which is given by

$$\frac{r_t}{r_o} = 1 + \alpha\left[t - \delta\left(\frac{t}{100} - 1\right)\frac{t}{100} - \beta\left(\frac{t}{100} - 1\right)\left(\frac{t}{100}\right)^3\right] \tag{A-2}$$

where:

r_t resistance (in ohms) at temperature t ($^\circ$C) of the blackbody target

r_o resistance at t = 0°C (supplied by the manufacturer via Aerojet)

β 0 for t > 0°C, and 0.11 for t < 0°

α and δ are constants provided by the manufacturer via Aerojet.

Calculation shows that the error is negligible by setting $\beta = 0$ in Equation (A-2). In this study, it is assumed $\beta = 0$ in all cases, then Equation (A-2) is simplified into a quadratic equation in t. In such case, one can solve the quadratic equation for t in terms of r_t. Then the PRT temperature in degree Kelvin is obtained from t + 273.15. By this way, data sets of PRT temperatures versus counts for individual PRTs are computed. Then Equation (1) is applied to fit these data sets for obtaining the polynomial coefficients f_{kj} for individual PRTs and housekeeping sensors. These best-fit coefficients are listed in Tables A-1 and A-2, respectively, for AMSU-A1 SN 106 and AMSU-A2 SN 108. Test calculations show that these polynomials are very accurate in reproducing temperatures of all sensors with errors in order of 0.01 K.

Table A-1. METOP-A AMSU-A1 SN 106: Coefficients for converting PRT counts into temperatures.

PRT	f_{k0}	f_{k1}	f_{k2}	f_{k3}	Description
1	263.9870	1.731689E-03	3.822561E-09	1.028422E-14	Al-1 MOTOR
2	263.9702	1.733920E-03	3.767659E-09	1.082943E-14	A 1-2 MOTOR
3	262.9015	1.733436E-03	3.664060E-09	1.218533E-14	A 1-1 FEED HORN
4	263.6334	1.735609E-03	3.725756E-09	1.052431E-14	A 1-2 FEED HORN
5	262.9389	1.731870E-03	3.623842E-09	1.211609E-14	Al-I RFMUX
6	263.4331	1.735790E-03	3.669909E-09	1.211365E-14	A]-2RFMUX
7	263.5560	1.735983E-03	3.967947E-09	7.681595E-15	CH. 3 DRO
8	262.9373	1.734014E-03	3.761015E-09	1.121131E-14	CH. 4 DRO
9	262.8178	1.731163E-03	3.752029E-09	9.505904E-15	CH. 5 DRO
10	263.4417	1.734077E-03	3.917796E-09	1.128447E-14	CH. 6 DRO
11	262.9996	1.747369E-03	3.343567E-09	9.155990E-15	CH. 7 DRO
12	263.3053	1.741015E-03	3.500605E-09	1.183477E-14	CH. 8 DRO
13	263.6873	1.736346E-03	3.610864E-09	1.205842E-14	CH. 15 GDO
14	263.3672	1.735200E-03	3.709033E-09	1.101641E-14	CH. 9 thru 14 PLO #2
15	263.6137	1.733371E-03	3.764484E-09	9.452957E-15	CH. 9 thru 14 PLO #1
16	263.6137	1.733371E-03	3.764484E-09	9.452957E-15	Not Used(Dummy Nu.)
17	264.0699	1.734028E-03	3.767572E-09	9.111964E-15	CH. 3 MIXER/IF
18	263.9319	1.748879E-03	3.388072E-09	9.858423E-15	CH. 4 MIXERAF
19	263.6916	1.745153E-03	3.560328E-09	8.698514E-15	CH. 5 MIXERAF
20	262.6377	1.723487E-03	3.583203E-09	1.212495E-14	CH. 6 MIXER/IF
21	263.6421	1.738316E-03	3.631971E-09	1.190380E-14	CH. 7 MlXER/IF
22	263.4369	1.743099E-03	3.495317E-09	1.188741E-14	CH. 8 MIXER/IF
23	262.7352	1.728822E-03	3.735996E-09	1.120497E-14	CH.9 thru 14 MIXERAF
24	262.9482	1.731860E-03	3.694364E-09	1.190977E-14	CH. 15 MIXER/IF
25	263.2314	1.732163E-03	3.762795E-09	9.773389E-15	CH. 11 thru 14 IF AMP
26	263.0380	1.741121E-03	3.748129E-09	9.851083E-15	CH. 9 IF AMP
27	263.3186	1.742946E-03	3.730115E-09	1.125205E-14	CH. 10 IF AMP
28	264.0114	1.742906E-03	3.647763E-09	1.123192E-14	CH. I I IF AMP
29	262.9898	1.726485E-03	3.956736E-09	1.243824E-14	DC/DC CONVERTER
30	263.5477	1.733392E-03	3.646014E-09	1.166024E-14	CH. 13 IF AMP
31	263.2184	1.740073E-03	3.755627E-09	1.069445E-14	CH. 14 IF AMP
32	263.2916	1.732509E-03	3.836888E-09	9.925257E-15	CH. 12 IF AMP
33	263.6981	1.731287E-03	3.778609E-09	9.565021E-15	Al-1 RFSHELF
34	264.3354	1.748171E-03	3.357364E-09	1.082636E-14	Al-2 RF SHELF
35	263.7312	1.736234E-03	3.693059E-09	1.127579E-14	DETECTOR/PRE-AMP
36	254.5321	1.639002E-03	5.869509E-09	3.072612E-14	Al-1 WARM LOAD 1
37	254.0022	1.607209E-03	8.022662E-09	-2.009460E-14	Al-1 WARM LOAD 2
38	254.2602	1.644751E-03	5.892945E-09	3.041434E-14	Al-1 WARM LOAD 3
39	255.1122	1.608134E-03	6.005212E-09	3.373968E-14	Al-1 WARM LOAD 4
40	254.8325	1.635428E-03	5.877971E-09	3.002280E-14	A1-1 WARM LD CTR
41	254.4281	1.633255E-03	5.821995E-09	3.044200E-14	A1-2 WARM LOAD 1
42	254.4755	1.640935E-03	5.779129E-09	3.013209E-14	Al-2 WARM LOAD 2
43	254.2934	1.634954E-03	5.864132E-09	3.073197E-14	A1-2 WARM LOAD 3
44	254.5471	1.635103E-03	5.858410E-09	3.093710E-14	A1-2 WARM LOAD 4
45	254.6261	1.639420E-03	5.849467E-09	3.133734E-14	A1-2 WARM LOAD CTR

Table A-2. METOP AMSU-A2 SN 108: Polynomial coefficients for converting PRT counts into temperatures.

PRT	f_{k0}	f_{k1}	f_{k2}	f_{k3}	Description
1	263.1324	1.746917E-03	3.795735E-09	1.231495E-14	Scan Motor
2	263.3740	1.749617E-03	3.831857E-09	1.103431E-14	Feedhorn
3	264.3925	1.753566E-03	3.744340E-09	1.018223E-14	RF Diplexer
4	263.1567	1.749016E-03	3.802419E-09	1.137400E-14	Mixer/IF CH1
5	263.1198	1.756348E-03	3.787283E-09	1.159493E-14	Mixer/IF CH2
6	263.5626	1.748585E-03	3.751691E-09	1.205580E-14	CH 1 DRO
7	263.9182	1.751247E-03	3.825043E-09	9.937291E-15	CH 2 DRO
8	264.3978	1.745011E-03	4.094067E-09	1.029310E-14	Compensat Motor
9	263.4419	1.747650E-03	3.750830E-09	1.029786E-14	Sub Reflector
10	263.3896	1.748861E-03	3.783287E-09	1.118430E-14	DC/DC Converter
1	263.2304	1.743369E-03	3.927309E-09	1.077412E-14	RF Shelf
12	263.5447	1.746484E-03	3.886169E-09	8.975719E-15	Det. Pre-Amp
13	254.7548	1.647906E-03	5.906964E-09	3.154537E-14	Warm Load Ctr
14	254.7590	1.646893E-03	5.917976E-09	3.057754E-14	Warm Load #1
15	254.7516	1.651416E-03	5.905144E-09	2.987418E-14	Warm Load #2
16	254.5520	1.657917E-03	5.767012E-09	2.812747E-14	Warm Load #3
17	254.6245	1.640567E-03	5.931309E-09	3.082734E-14	Warm Load #4
18	254.5462	1.642780E-03	5.836231E-09	3.181955E-14	Warm Load #5
19	254.6566	1.658447E-03	5.775657E-09	3.352912E-14	Warm Load #6

A.2 *Warm Load Correction*

The in-flight warm load correction (WLC) was calculated according to a formula developed by Aerojet [6-9]. For each AMSU-A antenna system, a special set of calibration data were acquired by setting the temperature of its variable scene target equal to that of the internal blackbody (warm) target. The physical temperature T_W of the internal blackbody target was determined from the PRT counts as described in Section 2. The radiometric temperature T_{wrad} of the blackbody (in-flight warm load) was calculated (for each scan in the data set) by the formula

$$T_{wrad} = T_{sprt} + \left(T_{sprt} - T_C\right)\left(\frac{C_W - C_S}{C_S - C_C}\right) \tag{A-3}$$

where:

T_{sprt} PRT temperature of the variable scene target,

T_C PRT temperature of the cold target,

C_W the average of two radiometric counts from the warm target,

C_C the average of two radiometric counts from the cold target, and

C_S radiometric counts from the variable scene target.

One should note that temperatures, T_{sprt} and T_C, from the scene and cold targets are used as the two reference calibration points in Equation (A-3) to calculate the radiometric temperature of the warm target. The in-flight warm load correction factor ΔT_W was computed from the formula,

$$\Delta T_W = \frac{1}{N}\left[\sum_{i=1}^{N}\left(T_{wrad} - T_W\right)_i\right] \tag{A-4}$$

where N represents the number of scans in a data set. The ΔT_W values at three instrument (RF Shelf) temperatures for each AMSU-A antenna system are listed in Table A-3. For AMSU-A1, the ΔT_W values for both PLLO#1 and PPLO#2 were calculated and listed. These ΔT_W values will be used in both NOAA and METOP-A AMSU-A operational calibration algorithms.

A.3 *Nonlinearity parameters*

The nonlinearity is discussed in Section 4.2 and the values of the nonlinearity parameter u are listed in Table 4.

Table A-3. METOP-A AMSU-A warm load corrections (K) at three instrument temperatures.

AMSU-A2 SN 108 Channels AMSU-A1 SN 106 Channels

Instrument Temp.(C)	Ch. 1	Ch. 2	Instrument Temp.(C)	Ch. 3	Ch. 4	Ch. 5	Ch.8
6.91	0.017	-0.047	-2.57	-0.051	-0.049	-0.065	-0.059
11.81	0.006	-0.113	18.53	-0.059	-0.065	-0.087	-0.078
29.29	-0.045	-0.148	38.41	-0.177	-0.205	-0.169	-0.147

AMSU-A1-1 SN 106 Channels: PLLO#1:

Instrument Temp.(C)	Ch. 6	Ch. 7	Ch. 9	Ch. 10	Ch. 11	Ch. 12	Ch. 13	Ch. 14	Ch. 15
-2.35	0.262	0.283	0.240	0.267	0.283	0.235	0.213	0.211	0.258
18.57	0.324	0.333	0.264	0.329	0.309	0.300	0.275	0.267	0.293
37.88	0.273	0.289	0.268	0.239	0.244	0.234	0.261	0.263	0.233

AMSU-A1-1 SN 106 Channels: PLLO#2:

Instrument Temp.(C)	Ch. 9	Ch. 10	Ch. 11	Ch. 12	Ch. 13	Ch. 14
-2.36	0.067	0.139	0.143	0.085	0.100	0.049
18.69	0.289	0.305	0.284	0.268	0.302	0.190
37.91	0.302	0.207	0.193	0.146	0.179	0.243

A.4 *Correction to In-orbit Cold Space Calibration*

For on-orbit cold space calibration, there is an uncertainty due to antenna side lobe interference with the Earth limb and spacecraft. The contribution from this uncertainty should be added to the cold space cosmic background temperature of 2.73K. Therefore, the "effective " cold space temperature T_{EC} can be represented by

$$T_{EC} = 2.73 + \Delta T_C \tag{A-5}$$

where ΔT_C represents the contribution from the antenna side-lobe interference with the Earth limb and spacecraft. Estimates of ΔT_C for individual channels of METOP AMSU-A are made from the measured antenna pattern data [10]. These estimated ΔT_C values for the four available cold calibration positions are listed in Table A-4.

Table A-4. Values of METOP-A AMSU-A cold bias ΔT_C.

Pos. ID	Angle[a]	Ch. 1	Ch. 1	Ch. 3	Ch. 4	Ch. 5	Ch. 6	Ch. 7	Ch. 8	Ch. 9-14	Ch. 15
1	83.333	0.76	0.57	1.67	1.64	1.60	1.06	1.50	2.39	1.72	0.41
2	81.667	0.79	0.58	1.76	1.73	1.68	1.10	1.57	2.46	1.77	0.41
3	80.000	0.82	0.60	1.85	1.80	1.74	1.13	1.63	2.53	1.82	0.42
4	76.667	0.88	0.65	2.05	1.93	1.85	1.22	1.75	2.66	1.91	0.44

[a] Measured from nadir.

A.5 *Limit of Blackbody and Cold Counts Variation*

For each scan, the blackbody counts C_W is the average of two samples. If the two samples of the blackbody differ by more than a pre-set limit of blackbody count variation ΔC_W, the data in the scan will not be used. The ΔC_W values for individual channels are listed in Table A-5. These ΔC_W values, which equal approximately 3σ (where σ is the standard deviation of the internal blackbody counts), are calculated from the TV calibration data. Similarly, the cold count is the same.

Table A-5. METOP-A: Error Limits of Warm and cold radiometric counts between samples of same scan line.

Limit	Ch.1	2	3	4	5	6	7	8	9	10	11	12	13	14	15
Warm	18	18	18	18	18	18	18	18	18	18	24	24	30	60	22
Cold	18	18	18	18	18	18	18	18	18	18	24	24	30	60	22

A.6 *Pre-launch Determined Weight Factors w_k for the Internal Blackbody PRTs*

The weight factors w_k (see Equation 2) assigned to individual PRTs in the internal blackbody targets are listed in Table A-6. All METOP-A AMSU-A PRTs are good.

Table A-6. Pre-launch determined weight factors w_k assigned to METOP-A AMSU-A PRTs in blackbody targets.

Antenna System	w_1	w_2	w_3	w_4	w_5	w_6	w_7
AMSU-A2	1	1	1	1	1	1	1
AMSU-A1-1	1	1	1	1	1		
AMSU-A1-2	1	1	1	1	1		

A.7 *Conversion Coefficients of Analog Data*

AMSU-A instrument has an analog telemetry bus to monitor key temperatures and voltages through the spacecraft. The resolutions of the analog telemetry received on the ground is 20 mV for one part in 256. To convert the analog data into physical quantities y, one must multiply the analog values by 0. 02V (20 mV) to obtain the measured output, x, in volts and then uses the conversion equation,

$$y = B + M x \tag{A-6}$$

where the values of B and M are given in Tables A-7 and A-8 for METOP-A AMSU-A2 SN 108 and AMSU-A1 SN 106, respectively.

Table A-7. METOP-A AMSU-A2 SN 108: Analog data conversion coefficients.

UIIS Ref.	Description	y	M	B
1	Scanner Motor Temperature	K	68.027	0
2	Comp Motor Temperature	K	68.027	0
3	R.F. Shelf Temperature	K	68.027	0
4	Warm Load Temperature	c	68.027	0
5	Comp. Motor Current (average)	mA	46.6	0
6	Ant Drive Motor Current (ave)	mA	46.6	0
7	Signal Processing +15Vdc	v	4.315	0
8	Antenna Drive +15Vdc	v	4.315	0
9	Signal Processing -1 5Vdc	v	2.504	-22.562
10	Antenna Drive - 15Vdc	V	2.504	-22.562
11	Mixer/IF Amplifier +10 Vdc	V	2.889	0
12	Signal Processing +5Vdc	V	1.667	0
13	Antenna Drive +5Vdc	V	1.667	0
14	Local Oscillator +lOVdc. (ch.1)	V	2.861	0
15	Local Oscillator +lOVdc (ch.2)	V	2.861	0

Table A-8. METOP-A AMSU-A1 SN 106: Analog data conversion coefficients.

Pin #	**Description**	**y**	**M**	**B**
3	Al-1 Scanner Motor Temperature	K	68.027	0
22	A1-2 Scanner Motor Temperature	K	68.027	0
2	A1-1 RF Shelf Temperature	K	68.027	0
21	Al-2 RF Shelf Temperature	K	68.027	0
4	Al-1 Warm Load Temperature	K	68.027	0
23	Al-2 Warm Load Temperature	K	68.027	0
8	Al-1 Antenna Drive Motor Current	mA	23.3	0
27	Al-2 Antenna Drive Motor Current	mA	23.3	0
11	Signal Processing (+15 VDC)	v	4.315	0
9	Antenna Drive (+15 VDC)	v	4.315	0
29	Signal Processing (-15 VDC)	v	2.504	-22.562
28	Antenna Drive (-15 VDC)	v	2.504	-22.562
34	Receiver Amplifiers (+8 VDC)	v	2.50	0
12	Signal Processing (+5 VDC)	v	1.667	0
10	Antenna Drive (+5 VDC)	v	1.667	0
17	Receiver Mixer/IF (+10 VDC)	v	2.889	0
16	Phase Lock Loop Ch 9/14 (+15 VDC)	v	4.315	0
33	Phase Lock Loop Ch 9/14 (-15 VDC)	v	2.504	-22.562
13	Ch 3 L.O. Voltage (50.3 GHz)	v	2.861	0
30	Ch 4 L.O. Voltage (52.8 GHz)	v	2.861	0
14	Ch 5 L.O. Voltage (53.596 GHz)	v	2.861	0
31	Ch 6 L.O. Voltage (54.4 GHz)	v	2.861	0
15	Ch 7 L.O. Voltage (54.94 GHz)	v	2.861	0
32	Ch 8 L.O. Voltage (55.5 GHz)	v	2.861	0
25	PLLO Primary Lock Detect (PLO #1)	v	1.0	0
6	PLLO Redundant Lock Detect (PLO #2)	v	1.0	0
18	Ch 15 L.O. Voltage (89.0 GHz)	v	4.315	0

APPENDIX B

NOAA POLAR ORBITER LEVEL 1B DATA

The NOAA Polar Orbiter Level 1B data are raw data that have been quality controlled and assembled into discrete data sets, to which Earth location and calibration information are appended but not applied. For simplification of application, the conversion of scene counts C_S into scene radiance R_S is accomplished by writing Equation (4) as

$$R_S = a_0 + a_1 C_S + a_2 C_S^2 \qquad \text{(B-1)}$$

where the calibration coefficients a_i (where i = 0, 1, and 2), which are output in the 1B data sets for individual scans, are expressed in terms of averaged calibration counts (over 7 scans) and calibration target temperatures. Derivation of these coefficients is described in the *NOAA KLM User's Guide*. In Equation (B-1), there is a quadratic term which represents the nonlinearities in the measurements [1]. Users, who prefer scene temperature instead of radiance, can make the simple conversion,

$$T_S = B^{-1}\left(R_S\right) \qquad \text{(B-2)}$$

where $B^{-1}(R_S)$ is the inverse of the Planck function for radiance R_S. The T_S is the converted antenna scene temperature.

The above calibration process applies to all AMSU-A measurements from NOAA-15, -16, -17, and -18.

NESDIS 103 GOES-11 Imager and Sounder Radiance and Product Validations for the GOES-11 Science Test. Jaime M. Daniels and Timothy J. Schmit, August 2001.

NESDIS 104 Summary of the NOAA/NESDIS Workshop on Development of a Coordinated Coral Reef Research and Monitoring Program. Jill E. Meyer and H. Lee Dantzler, August 2001.

NESDIS 105 Validation of SSM/I and AMSU Derived Tropical Rainfall Potential (TRaP) During the 2001 Atlantic Hurricane Season. Ralph Ferraro, Paul Pellegrino, Sheldon Kusselson, Michael Turk, and Stan Kidder, August 2002.

NESDIS 106 Calibration of the Advanced Microwave Sounding Unit-A Radiometers for NOAA-N and NOAA-N'. Tsan Mo, September 2002.

NESDIS 107 NOAA Operational Sounding Products for Advanced-TOVS: 2002. Anthony L. Reale, Micheal W. Chalfant, Americo S. Allergrino, Franklin H. Tilley, Michael P. Ferguson, and Michael E. Pettey, December 2002.

NESDIS 108 Analytic Formulas for the Aliasing of Sea Level Sampled by a Single Exact-Repeat Altimetric Satellite or a Coordinated Constellation of Satellites. Chang-Kou Tai, November 2002.

NESDIS 109 Description of the System to Nowcast Salinity, Temperature and Sea nettle (*Chrysaora quinquecirrha*) Presence in Chesapeake Bay Using the Curvilinear Hydrodynamics in 3-Dimensions (CH3D) Model. Zhen Li, Thomas F. Gross, and Christopher W. Brown, December 2002.

NESDIS 110 An Algorithm for Correction of Navigation Errors in AMSU-A Data. Seiichiro Kigawa and Michael P. Weinreb, December 2002.

NESDIS 111 An Algorithm for Correction of Lunar Contamination in AMSU-A Data. Seiichiro Kigawa and Tsan Mo, December 2002.

NESDIS 112 Sampling Errors of the Global Mean Sea Level Derived from Topex/Poseidon Altimetry. Chang-Kou Tai and Carl Wagner, December 2002.

NESDIS 113 Proceedings of the International GODAR Review Meeting: Abstracts. Sponsors: Intergovernmental Oceanographic Commission, U.S. National Oceanic and Atmospheric Administration, and the European Community, May 2003.

NESDIS 114 Satellite Rainfall Estimation Over South America: Evaluation of Two Major Events. Daniel A. Vila, Roderick A. Scofield, Robert J. Kuligowski, and J. Clay Davenport, May 2003.

NESDIS 115 Imager and Sounder Radiance and Product Validations for the GOES-12 Science Test. Donald W. Hillger, Timothy J. Schmit, and Jamie M. Daniels, September 2003.

NESDIS 116 Microwave Humidity Sounder Calibration Algorithm. Tsan Mo and Kenneth Jarva, October 2004.

NESDIS 117 Building Ocean Profile-Plankton Databases for Climate and Ecosystem Research. Sydney Levitus, Satoshi Sato, Catherine Maillard, Nick Mikhailov, Pat Caldwell, and Harry Dooley (Retired), June 2005.

NESDIS 118 Simultaneous Nadir Overpasses for NOAA-6 to NOAA-17 Satellites from 1980 to 2003 for the Intersatellite Calibration of Radiometers. Changyong Cao, Mitch Goldberg, Fuzhong Weng, Cheng-Zhi Zou, and Pubu Ciren, August 2005.

NESDIS 119 Calibration and Validation of NOAA-18 Instruments. Fuzhong Weng and Tsan Mo, December 2005.

NESDIS 120 THE NOAA/NESDIS/ORA WindSat Calibration/Validation Collocation Database. Larry Connor, February 2006.

NOAA SCIENTIFIC AND TECHNICAL PUBLICATIONS

The National Oceanic and Atmospheric Administration **was established as part of the Department of Commerce on October 3, 1970. The mission responsibilities of NOAA are to assess the socioeconomic impact of natural and technological changes in the environment and to monitor and predict the state of the solid Earth, the oceans and their living resources, the atmosphere, and the space environment of the Earth.**

The major components of NOAA regularly produce various types of scientific and technical information in the following types of publications:

PROFESSIONAL PAPERS - Important definitive research results, major techniques, and special investigations.

CONTRACT AND GRANT REPORTS - Reports prepared by contractors or grantees under NOAA sponsorship.

ATLAS - Presentation of analyzed data generally in the form of maps showing distribution of rainfall, chemical and physical conditions of oceans and atmosphere, distribution of fishes and marine mammals, ionospheric conditions, etc.

TECHNICAL SERVICE PUBLICATIONS - Reports containing data, observations, instructions, etc. A partial listing includes data serials; prediction and outlook periodicals; technical manuals, training papers, planning reports, and information serials; and miscellaneous technical publications.

TECHNICAL REPORTS - Journal quality with extensive details, mathematical developments, or data listings.

TECHNICAL MEMORANDUMS - Reports of preliminary, partial, or negative research or technology results, interim instructions, and the like.

U.S. DEPARTMENT OF COMMERCE
National Oceanic and Atmospheric Administration
National Environmental Satellite, Data, and Information Service
Washington, D.C. 20233